PIER M

(Received 25 April 2023, Accepted 10 January 2024, Scheduled 23 January 2024)

Relaxation of the Courant Condition in the Explicit Finite-Difference Time-Domain (2,6) Method with Third- and Fifth-Degree Differential Terms

Harune Sekido* and Takayuki Umeda

Institute for Space-Earth Environmental Research, Nagoya University, Japan.

ABSTRACT: A new non-dissipative and explicit finite-difference time-domain (FDTD) method is proposed for relaxation of the Courant condition of FDTD(2,6) in three and two dimensions. To the time-development equations, the third- and fifth-degree spatial difference terms with fourth- and second-order accuracy, respectively, are appended with coefficients. A set of optimal coefficients for the appended terms is searched to minimize the numerical error in phase velocity but relax the Courant condition as well. The numerical errors with the new method are more reduced than those with the previous methods for each Courant number. However, there exists a large anisotropy in the phase velocity errors at large Courant numbers.

1. INTRODUCTION

The Finite-Difference Time-Domain (FDTD) method has been widely used as a method for numerical simulations of electromagnetic fields for more than a half century [1, 2]. The FDTD method consists of the time-development equations of electric and magnetic fields based on Maxwell's equations. The time-development equations are discretized with the second-order finite difference in both time and space. The divergence free condition for both electric and magnetic fields is always satisfied in the staggered grid (Yee grid) system.

As a disadvantage of the FDTD method, phase velocity errors cause numerical oscillations due to lower-order finite differences. Finite differences with a higher-order accuracy are used for the reduction of phase velocity errors. With the FDTD(2,4) method, spatial difference terms are approximated with the fourth-order difference [3, 4]. The sixth-order spatial difference is used in the time-development equations of FDTD(2,6) in the same way. The FDTD method with the tth- and xth-order accuracies in time and space, respectively, is called FDTD(t, x).

By performing Fourier transform of the time-development equations and by setting the determinant to zero, the dispersion relation is obtained as a matrix eigenvalue problem [5, 6]. Then, the Courant condition is obtained from the dispersion relation. The dispersion relation of FDTD(2,6) is written as follows:

$$\mathcal{W}^2 = \left\{C_x\left(\mathcal{K}_x + \frac{1}{6}\mathcal{K}_x^3 + \frac{3}{40}\mathcal{K}_x^5\right)\right\}^2 + \left\{C_y\left(\mathcal{K}_y + \frac{1}{6}\mathcal{K}_y^3 + \frac{3}{40}\mathcal{K}_y^5\right)\right\}^2 + \left\{C_z\left(\mathcal{K}_z + \frac{1}{6}\mathcal{K}_z^3 + \frac{3}{40}\mathcal{K}_z^5\right)\right\}^2. \quad (1)$$

Here, the Courant numbers are defined as $C_x = c\Delta t/\Delta x$, $C_y = c\Delta t/\Delta y$ and $C_z = c\Delta t/\Delta z$. Numerical frequency and wavenumber are defined as $\mathcal{W} = \sin(\omega\Delta t/2)$ and $\mathcal{K}_x = \sin(k_x\Delta x/2)$, respectively. Note that $\mathcal{K}_z = 0$ in two dimensions. In n dimensions, the right-hand side of Eq. (1) is maximized at $k\Delta x = k\Delta y = k\Delta z = \pi$:

$$\mathcal{W}^2 = n\left(\frac{149}{120}C\right)^2,$$

where $C = C_x = C_y = C_z$ (i.e., $\Delta x = \Delta y = \Delta z$) is assumed. Therefore, a numerical instability occurs if the right-hand side of Eq. (1) is more than 1 (i.e., $C \geq 120/149\sqrt{2} \sim 0.57$ and $C \geq 120/149\sqrt{3} \sim 0.46$ in two and three dimensions, respectively). Note that the numerical instability occurs for $C > 1/\sqrt{3} \sim 0.577$ and $C > 6/7\sqrt{3} \sim 0.495$ with FDTD(2,2) and FDTD(2,4), respectively, in three dimensions.

The phase velocity errors with FDTD($2, x$) schemes ($x = 2, 4, 6, 8$) decrease as the order of the spatial difference increases [7]. However, the Courant condition becomes more restricted by using higher-order finite differences in space. Since FDTD(2,6) has a more restrictive Courant condition than FDTD(2,4), smaller Δt and larger number of time steps are required. For this reason, FDTD(2,6) is not used commonly.

Implicit FDTD methods [8–14] relax the Courant condition. Since the implicit equations need to be solved with iterative convergence or matrix inversion, they have higher computational costs. Nonstandard-type FDTD methods [15–20] utilize diagonal difference terms with coefficients to correct the numerical dispersion relation and to reduce phase velocity errors. However, it is not easy to obtain optimal coefficients of the appended terms.

* Corresponding author: Harune Sekido (sekido@isee.nagoya-u.ac.jp).

Recently, an explicit method for relaxing the Courant condition has been developed [21]. For the derivation of the time-development equations of this method, the third-degree difference terms are appended to FDTD(2,4) with coefficients. Optimal coefficients are determined by a brute-force search, which minimize the mean values of the phase velocity errors in the entire wavenumber space.

In this paper, the Courant condition of FDTD(2,6) is relaxed in the same way as the previous study [21]. A new FDTD method, which is non-dissipative and explicit, is developed by appending third- and fifth-degree difference terms to the time-development equations of FDTD(2,6).

This paper is organized as follows. Section 2 shows the time-development equations and the numerical dispersion relations of the new method. Section 3 shows the optimal coefficients and phase velocity errors. Section 4 shows the results of numerical tests. Section 5 gives the conclusion.

2. FORMULATION AND NUMERICAL DISPERSION RELATION

2.1. General Form

The following time-development equations are used, in which third- and fifth-degree spatial difference terms are appended:

$$
\begin{aligned}
B_x^{t+\frac{\Delta t}{2}}\left(x,y+\frac{\Delta y}{2},z+\frac{\Delta z}{2}\right) &= B_x^{t-\frac{\Delta t}{2}}\left(x,y+\frac{\Delta y}{2},z+\frac{\Delta z}{2}\right) \\
&-\mathcal{D}_y^1 E_z^t\left(x,y+\frac{\Delta y}{2},z+\frac{\Delta z}{2}\right)-\alpha\mathcal{D}_y^3 E_z^t\left(x,y+\frac{\Delta y}{2},z+\frac{\Delta z}{2}\right) \\
&-\beta\mathcal{D}_y^5 E_z^t\left(x,y+\frac{\Delta y}{2},z+\frac{\Delta z}{2}\right)+\mathcal{D}_z^1 E_y^t\left(x,y+\frac{\Delta y}{2},z+\frac{\Delta z}{2}\right) \\
&+\alpha\mathcal{D}_z^3 E_y^t\left(x,y+\frac{\Delta y}{2},z+\frac{\Delta z}{2}\right) \\
&+\beta\mathcal{D}_z^5 E_y^t\left(x,y+\frac{\Delta y}{2},z+\frac{\Delta z}{2}\right) \qquad (2a)
\end{aligned}
$$

$$
\begin{aligned}
E_x^{t+\Delta t}\left(x+\frac{\Delta x}{2},y,z\right) &= E_x^t\left(x+\frac{\Delta x}{2},y,z\right) \\
&+c^2\mathcal{D}_y^1 B_z^{t+\frac{\Delta t}{2}}\left(x+\frac{\Delta x}{2},y,z\right)+c^2\alpha\mathcal{D}_y^3 B_z^{t+\frac{\Delta t}{2}}\left(x+\frac{\Delta x}{2},y,z\right) \\
&+c^2\beta\mathcal{D}_y^5 B_z^{t+\frac{\Delta t}{2}}\left(x+\frac{\Delta x}{2},y,z\right) \\
&-c^2\mathcal{D}_z^1 B_y^{t+\frac{\Delta t}{2}}\left(x+\frac{\Delta x}{2},y,z\right) \\
&-c^2\alpha\mathcal{D}_z^3 B_y^{t+\frac{\Delta t}{2}}\left(x+\frac{\Delta x}{2},y,z\right) \\
&-c^2\beta\mathcal{D}_z^5 B_y^{t+\frac{\Delta t}{2}}\left(x+\frac{\Delta x}{2},y,z\right) \qquad (2b)
\end{aligned}
$$

$$
\begin{aligned}
B_y^{t+\frac{\Delta t}{2}}\left(x+\frac{\Delta x}{2},y,z+\frac{\Delta z}{2}\right) &= B_y^{t-\frac{\Delta t}{2}}\left(x+\frac{\Delta x}{2},y,z+\frac{\Delta z}{2}\right) \\
&-\mathcal{D}_z^1 E_x^t\left(x+\frac{\Delta x}{2},y,z+\frac{\Delta z}{2}\right) \\
&-\alpha\mathcal{D}_z^3 E_x^t\left(x+\frac{\Delta x}{2},y,z+\frac{\Delta z}{2}\right) \\
&-\beta\mathcal{D}_z^5 E_x^t\left(x+\frac{\Delta x}{2},y,z+\frac{\Delta z}{2}\right) \\
&+\mathcal{D}_x^1 E_z^t\left(x+\frac{\Delta x}{2},y,z+\frac{\Delta z}{2}\right) \\
&+\alpha\mathcal{D}_x^3 E_z^t\left(x+\frac{\Delta x}{2},y,z+\frac{\Delta z}{2}\right) \\
&+\beta\mathcal{D}_x^5 E_z^t\left(x+\frac{\Delta x}{2},y,z+\frac{\Delta z}{2}\right) \qquad (2c)
\end{aligned}
$$

$$
\begin{aligned}
E_y^{t+\Delta t}\left(x,y+\frac{\Delta y}{2},z\right) &= E_y^t\left(x,y+\frac{\Delta y}{2},z\right) \\
&+c^2\mathcal{D}_z^1 B_x^{t+\frac{\Delta t}{2}}\left(x,y+\frac{\Delta y}{2},z\right) \\
&+\alpha c^2\mathcal{D}_z^3 B_x^{t+\frac{\Delta t}{2}}\left(x,y+\frac{\Delta y}{2},z\right) \\
&+\beta c^2\mathcal{D}_z^5 B_x^{t+\frac{\Delta t}{2}}\left(x,y+\frac{\Delta y}{2},z\right) \\
&-c^2\mathcal{D}_x^1 B_z^{t+\frac{\Delta t}{2}}\left(x,y+\frac{\Delta y}{2},z\right) \\
&-\alpha c^2\mathcal{D}_x^3 B_z^{t+\frac{\Delta t}{2}}\left(x,y+\frac{\Delta y}{2},z\right) \\
&-\beta c^2\mathcal{D}_x^5 B_z^{t+\frac{\Delta t}{2}}\left(x,y+\frac{\Delta y}{2},z\right) \qquad (2d)
\end{aligned}
$$

$$
\begin{aligned}
B_z^{t+\frac{\Delta t}{2}}\left(x+\frac{\Delta x}{2},y+\frac{\Delta y}{2},z\right) &= B_z^{t-\frac{\Delta t}{2}}\left(x+\frac{\Delta x}{2},y+\frac{\Delta y}{2},z\right) \\
&-\mathcal{D}_x^1 E_y^t\left(x+\frac{\Delta x}{2},y+\frac{\Delta y}{2},z\right) \\
&-\alpha\mathcal{D}_x^3 E_y^t\left(x+\frac{\Delta x}{2},y+\frac{\Delta y}{2},z\right) \\
&-\beta\mathcal{D}_x^5 E_y^t\left(x+\frac{\Delta x}{2},y+\frac{\Delta y}{2},z\right) \\
&+\mathcal{D}_y^1 E_x^t\left(x+\frac{\Delta x}{2},y+\frac{\Delta y}{2},z\right) \\
&+\alpha\mathcal{D}_y^3 E_x^t\left(x+\frac{\Delta x}{2},y+\frac{\Delta y}{2},z\right)
\end{aligned}
$$

$$+\beta\mathcal{D}_y^5 E_x^t\left(x+\frac{\Delta x}{2},y+\frac{\Delta y}{2},z\right) \tag{2e}$$

$$E_z^{t+\Delta t}\left(x,y,z+\frac{\Delta z}{2}\right)=E_z^t\left(x,y,z+\frac{\Delta z}{2}\right)$$

$$+c^2\mathcal{D}_x^1 B_y^{t+\frac{\Delta t}{2}}\left(x,y,z+\frac{\Delta z}{2}\right)$$

$$+\alpha c^2\mathcal{D}_x^3 B_y^{t+\frac{\Delta t}{2}}\left(x,y,z+\frac{\Delta z}{2}\right)$$

$$+\beta c^2\mathcal{D}_x^5 B_y^{t+\frac{\Delta t}{2}}\left(x,y,z+\frac{\Delta z}{2}\right)$$

$$-c^2\mathcal{D}_y^1 B_x^{t+\frac{\Delta t}{2}}\left(x,y,z+\frac{\Delta z}{2}\right)$$

$$-\alpha c^2\mathcal{D}_y^3 B_x^{t+\frac{\Delta t}{2}}\left(x,y,z+\frac{\Delta z}{2}\right)$$

$$-\beta c^2\mathcal{D}_y^5 B_x^{t+\frac{\Delta t}{2}}\left(x,y,z+\frac{\Delta z}{2}\right) \tag{2f}$$

where c is the speed of light; α and β are coefficients with the third- and fifth-degree difference terms, respectively; and $\mathcal{D}_x^n$ is a nth-degree spatial difference operator. Note that $\mathcal{D}_z^n=0$ in two dimensions. A set of optimal coefficients is determined as a function of the Courant number. The time-development equations are based on the Taylor expansion of the central finite difference in time, which has odd-degree difference terms only. A numerical dissipation arises from even-degree difference terms.

2.2. FDTD(2,6) with Third-Degree Difference

The first-degree spatial difference operator $\mathcal{D}_x^1$ with sixth-order accuracy is written as follows:

$$\begin{aligned}&\mathcal{D}_x^1 E_y^t\left(x+\frac{\Delta x}{2},y+\frac{\Delta y}{2},z\right)\\ =\;&\frac{1}{1920}\frac{\Delta t}{\Delta x}\left\{9E_y^t\left(x+3\Delta x,y+\frac{\Delta y}{2},z\right)\right.\\ &-125E_y^t\left(x+2\Delta x,y+\frac{\Delta y}{2},z\right)\\ &+2250E_y^t\left(x+\Delta x,y+\frac{\Delta y}{2},z\right)\\ &-2250E_y^t\left(x,y+\frac{\Delta y}{2},z\right)\\ &+125E_y^t\left(x-\Delta x,y+\frac{\Delta y}{2},z\right)\\ &\left.-9E_y^t\left(x-2\Delta x,y+\frac{\Delta y}{2},z\right)\right\}.\end{aligned} \tag{3}$$

The third-degree difference operator $\mathcal{D}_x^3$ with fourth-order accuracy is written as follows:

$$\begin{aligned}&\mathcal{D}_x^3 E_y^t\left(x+\frac{\Delta x}{2},y+\frac{\Delta y}{2},z\right)\\ =\;&\frac{c^2}{8}\left(\frac{\Delta t}{\Delta x}\right)^3\left\{-E_y^t\left(x+3\Delta x,y+\frac{\Delta y}{2},z\right)\right.\\ &+13E_y^t\left(x+2\Delta x,y+\frac{\Delta y}{2},z\right)\\ &-34E_y^t\left(x+\Delta x,y+\frac{\Delta y}{2},z\right)\\ &+34E_y^t\left(x,y+\frac{\Delta y}{2},z\right)-13E_y^t\left(x-\Delta x,y+\frac{\Delta y}{2},z\right)\\ &\left.+E_y^t\left(x-2\Delta x,y+\frac{\Delta y}{2},z\right)\right\}.\end{aligned} \tag{4}$$

The dispersion relation is derived from Eqs. (2), (3), and (4) with $\mathcal{D}_x^5=0$ as follows:

$$\begin{aligned}\mathcal{W}^2 \;=\;&\alpha^2\left\{16\left(C_x^6\mathcal{K}_x^6+C_y^6\mathcal{K}_y^6+C_z^6\mathcal{K}_z^6\right)\right.\\ &+16\left(C_x^6\mathcal{K}_x^8+C_y^6\mathcal{K}_y^8+C_z^6\mathcal{K}_z^8\right)\\ &\left.+4\left(C_x^6\mathcal{K}_x^{10}+C_y^6\mathcal{K}_y^{10}+C_z^6\mathcal{K}_z^{10}\right)\right\}\\ &-2\alpha\left\{4\left(C_x^4\mathcal{K}_x^4+C_y^4\mathcal{K}_y^4+C_z^4\mathcal{K}_z^4\right)\right.\\ &+\frac{8}{3}\left(C_x^4\mathcal{K}_x^6+C_y^4\mathcal{K}_y^6+C_z^4\mathcal{K}_z^6\right)\\ &+\frac{19}{30}\left(C_x^4\mathcal{K}_x^8+C_y^4\mathcal{K}_y^8+C_z^4\mathcal{K}_z^8\right)\\ &\left.+\frac{3}{20}\left(C_x^4\mathcal{K}_x^{10}+C_y^4\mathcal{K}_y^{10}+C_z^4\mathcal{K}_z^{10}\right)\right\}\\ &+\left\{\left(C_x^2\mathcal{K}_x^2+C_y^2\mathcal{K}_y^2+C_z^2\mathcal{K}_z^2\right)\right.\\ &+\frac{1}{3}\left(C_x^2\mathcal{K}_x^4+C_y^2\mathcal{K}_y^4+C_z^2\mathcal{K}_z^4\right)\\ &+\frac{8}{45}\left(C_x^2\mathcal{K}_x^6+C_y^2\mathcal{K}_y^6+C_z^2\mathcal{K}_z^6\right)\\ &+\frac{1}{40}\left(C_x^2\mathcal{K}_x^8+C_y^2\mathcal{K}_y^8+C_z^2\mathcal{K}_z^8\right)\\ &\left.+\frac{9}{1600}\left(C_x^2\mathcal{K}_x^{10}+C_y^2\mathcal{K}_y^{10}+C_z^2\mathcal{K}_z^{10}\right)\right\}.\end{aligned} \tag{5}$$

Note that $\mathcal{K}_z=0$ in two dimensions. The left-hand side takes a value in the range of $0\le\mathcal{W}^2\le 1$. The Courant condition is relaxed by adjusting the coefficient α.

This method is referred to as "scheme 1" in this paper.

2.3. FDTD(2,6) with Third- and Fifth-Degree Differences

The fifth-degree difference operator $\mathcal{D}_x^5$ with second-order accuracy is written as follows:

$$\begin{aligned}
&\mathcal{D}_x^5 E_y^t\left(x+\frac{\Delta x}{2}, y+\frac{\Delta y}{2}, z\right)\\
=\ & c^4\left(\frac{\Delta t}{\Delta x}\right)^5\left\{E_y^t\left(x+3\Delta x, y+\frac{\Delta y}{2}, z\right)\right.\\
&-5E_y^t\left(x+2\Delta x, y+\frac{\Delta y}{2}, z\right)\\
&+10E_y^t\left(x+\Delta x, y+\frac{\Delta y}{2}, z\right)\\
&-10E_y^t\left(x, y+\frac{\Delta y}{2}, z\right)+5E_y^t\left(x-\Delta x, y+\frac{\Delta y}{2}, z\right)\\
&\left.-E_y^t\left(x-2\Delta x, y+\frac{\Delta y}{2}, z\right)\right\}. \qquad (6)
\end{aligned}$$

The dispersion relation is derived from Eqs. (2), (3), (4), and (6) as follows:

$$\begin{aligned}
\mathcal{W}^2 =\ & 256\beta^2\left(C_x^{10}\mathcal{K}_x^{10}+C_y^{10}\mathcal{K}_y^{10}+C_z^{10}\mathcal{K}_z^{10}\right)\\
&-2\alpha\beta\left\{64\left(C_x^8\mathcal{K}_x^8+C_y^8\mathcal{K}_y^8+C_z^8\mathcal{K}_z^8\right)\right.\\
&+32\left(C_x^8\mathcal{K}_x^{10}+C_y^8\mathcal{K}_y^{10}+C_z^8\mathcal{K}_z^{10}\right)\}\\
&+\alpha^2\left\{16\left(C_x^6\mathcal{K}_x^6+C_y^6\mathcal{K}_y^6+C_z^6\mathcal{K}_z^6\right)\right.\\
&+16\left(C_x^6\mathcal{K}_x^8+C_y^6\mathcal{K}_y^8+C_z^6\mathcal{K}_z^8\right)\\
&+4\left(C_x^6\mathcal{K}_x^{10}+C_y^6\mathcal{K}_y^{10}+C_z^6\mathcal{K}_z^{10}\right)\}\\
&+2\beta\left\{16\left(C_x^6\mathcal{K}_x^6+C_y^6\mathcal{K}_y^6+C_z^6\mathcal{K}_z^6\right)\right.\\
&+\frac{8}{3}\left(C_x^6\mathcal{K}_x^8+C_y^6\mathcal{K}_y^8+C_z^6\mathcal{K}_z^8\right)\\
&\left.+\frac{6}{5}\left(C_x^6\mathcal{K}_x^{10}+C_y^6\mathcal{K}_y^{10}+C_z^6\mathcal{K}_z^{10}\right)\right\}\\
&-2\alpha\left\{4\left(C_x^4\mathcal{K}_x^4+C_y^4\mathcal{K}_y^4+C_z^4\mathcal{K}_z^4\right)\right.\\
&+\frac{8}{3}\left(C_x^4\mathcal{K}_x^6+C_y^4\mathcal{K}_y^6+C_z^4\mathcal{K}_z^6\right)\\
&+\frac{19}{30}\left(C_x^4\mathcal{K}_x^8+C_y^4\mathcal{K}_y^8+C_z^4\mathcal{K}_z^8\right)\\
&\left.+\frac{3}{20}\left(C_x^4\mathcal{K}_x^{10}+C_y^4\mathcal{K}_y^{10}+C_z^4\mathcal{K}_z^{10}\right)\right\}\\
&+\left\{\left(C_x^2\mathcal{K}_x^2+C_y^2\mathcal{K}_y^2+C_z^2\mathcal{K}_z^2\right)\right.\\
&+\frac{1}{3}\left(C_x^2\mathcal{K}_x^4+C_y^2\mathcal{K}_y^4+C_z^2\mathcal{K}_z^4\right)\\
&+\frac{8}{45}\left(C_x^2\mathcal{K}_x^6+C_y^2\mathcal{K}_y^6+C_z^2\mathcal{K}_z^6\right)\\
&+\frac{1}{40}\left(C_x^2\mathcal{K}_x^8+C_y^2\mathcal{K}_y^8+C_z^2\mathcal{K}_z^8\right)\\
&\left.+\frac{9}{1600}\left(C_x^2\mathcal{K}_x^{10}+C_y^2\mathcal{K}_y^{10}+C_z^2\mathcal{K}_z^{10}\right)\right\}. \qquad (7)
\end{aligned}$$

Note that $\mathcal{K}_z = 0$ in two dimensions. The Courant condition is relaxed by adjusting both α and β.

This method is referred to as "scheme 2" in this paper.

3. OPTIMAL COEFFICIENTS

A set of optimal coefficients for the third- and fifth-degree difference terms is obtained by a brute-force search as performed in the previous study [21]. The angular frequency ω is obtained by solving the dispersion relation. Here, $\omega = 2\sin^{-1}\mathcal{W}/\Delta t$ in Eq. (8) is obtained as a function of the numerical wavenumber $\mathcal{K}$ from Eqs. (5) and (7). The phase velocity is obtained by dividing the real part of angular frequency ω by wavenumber k. The coefficients are determined to minimize the phase velocity errors and suppress the numerical instabilities. The phase velocity error is given by the following equation:

$$\varepsilon = \frac{1}{c}\sqrt{\frac{\frac{\Delta x\Delta y\Delta z}{\pi^3}\int_0^{\pi/\Delta z}\int_0^{\pi/\Delta y}\int_0^{\pi/\Delta x}\left\{\frac{\omega}{\sqrt{k_x^2+k_y^2+k_z^2}}-c\right\}^2 \mathrm{d}k_x\mathrm{d}k_y\mathrm{d}k_z}{\frac{\Delta x\Delta y\Delta z}{\pi^3}\int_0^{\pi/\Delta z}\int_0^{\pi/\Delta y}\int_0^{\pi/\Delta x}\mathrm{d}k_x\mathrm{d}k_y\mathrm{d}k_z}}. \qquad (8)$$

The phase velocity error ε is obtained as a function of the coefficients α and β for a specific Courant number. In this study, $C = C_x = C_y = C_z$ (i.e., $\Delta x = \Delta y = \Delta z$) is assumed. A set of optimal coefficients α and β is searched for minimizing the error ε under the condition of $\mathrm{Im}(\omega) \le 0$.

In two dimensions, the optimal coefficients for schemes 1 and 2 are searched for $0.5 \le C \le 1$. Tables 1 and 2 show the sets of optimal coefficients for schemes 1 and 2 using Eqs. (5) and (7), respectively.

In three dimensions, the optimal coefficients for schemes 1 and 2 are searched for $0.4 \le C \le 1$. Tables 3 and 4 show the sets of optimal coefficients for schemes 1 and 2 using Eqs. (5) and (7), respectively.

3.1. Numerical Error in Two Dimensions

A method using the time-development equations with the fourth-order operator $\mathcal{D}_x^1$ and the second-order operator $\mathcal{D}_x^3$ is previously proposed [21], which is referred to as "Sekido23" in this paper.

The phase velocity errors of schemes 1 and 2 are compared with those of FDTD(2,6) and Sekido23 in two dimensions. Figure 1 shows the mean values of the phase velocity errors ε as a function of the Courant number C. Panels (a)–(c) show the phase velocity errors in the entire wavenumber space, at $\theta = 0°$ and at $\theta = 45°$, respectively. Here, θ is the angle relative to the x axis. The black, red, green, and blue lines show the numerical errors with FDTD(2,6), Sekido23, schemes 1 and 2 with the optimal coefficients in Tables 1 and 2, respectively.

TABLE 1. Optimal coefficients for scheme 1 in two dimensions.

C	α	C	α
0.50	0.0075	0.76	0.0899
0.51	0.0114	0.77	0.091
0.52	0.0152	0.78	0.0919
0.53	0.0188	0.79	0.0926
0.54	0.0222	0.80	0.0932
0.55	0.0256	0.81	0.0937
0.56	0.0289	0.82	0.0941
0.57	0.032	0.83	0.0943
0.58	0.0352	0.84	0.0945
0.59	0.0383	0.85	0.0946
0.60	0.0414	0.86	0.0946
0.61	0.0446	0.87	0.0945
0.62	0.0479	0.88	0.0943
0.63	0.0514	0.89	0.0941
0.64	0.0558	0.90	0.0939
0.65	0.0608	0.91	0.0936
0.66	0.0652	0.92	0.0932
0.67	0.0693	0.93	0.0928
0.68	0.0728	0.94	0.0924
0.69	0.076	0.95	0.0919
0.70	0.0788	0.96	0.0914
0.71	0.0813	0.97	0.0909
0.72	0.0835	0.98	0.0903
0.73	0.0855	0.99	0.0898
0.74	0.0871	1.00	0.0894
0.75	0.0886		

TABLE 2. Sets of optimal coefficients for scheme 2 in two dimensions.

C	α	β	C	α	β
0.50	0.2049	0.3304	0.76	−0.0351	−0.0812
0.51	0.1951	0.295	0.77	−0.0364	−0.0806
0.52	0.1856	0.2628	0.78	−0.0369	−0.0794
0.53	0.1763	0.2334	0.79	−0.0327	−0.0753
0.54	0.1672	0.2064	0.80	−0.0268	−0.0704
0.55	0.158	0.1813	0.81	−0.0218	−0.0662
0.56	0.1488	0.1579	0.82	−0.0135	−0.0602
0.57	0.1395	0.1361	0.83	−0.0069	−0.0553
0.58	0.1299	0.1154	0.84	−0.0029	−0.0521
0.59	0.1199	0.0956	0.85	0.0059	−0.0463
0.60	0.1096	0.0768	0.86	0.011	−0.0427
0.61	0.0984	0.0582	0.87	0.0159	−0.0393
0.62	0.0864	0.0398	0.88	0.0232	−0.0348
0.63	0.0733	0.0215	0.89	0.0265	−0.0325
0.64	0.0575	0.0015	0.90	0.0319	−0.0292
0.65	0.0423	−0.0165	0.91	0.0379	−0.0257
0.66	0.0279	−0.0322	0.92	0.045	−0.0218
0.67	0.0171	−0.0437	0.93	0.048	−0.0199
0.68	0.0053	−0.0548	0.94	0.0529	−0.0172
0.69	−0.0019	−0.0614	0.95	0.0561	−0.0154
0.70	−0.0092	−0.0674	0.96	0.0602	−0.0132
0.71	−0.0176	−0.0737	0.97	0.0641	−0.0112
0.72	−0.0224	−0.0767	0.98	0.0691	−0.0087
0.73	−0.0265	−0.0788	0.99	0.0752	−0.0059
0.74	−0.0316	−0.0814	1.00	0.0756	−0.0055
0.75	−0.0337	−0.0816			

The Courant conditions are relaxed for large Courant numbers where FDTD(2,6) is unstable. Panel (a) shows that the numerical errors of the present schemes are smaller than those of FDTD(2,6) for small Courant numbers. The numerical errors of the present schemes are smaller than or the same as those of Sekido23. The numerical errors of scheme 2 are smaller than those of the other schemes for all Courant numbers. Panels (b) and (c) show that the numerical errors at $\theta = 45°$ are smaller than those at $\theta = 0°$. Panel (b) shows that the numerical errors of schemes 1 and 2 at $\theta = 0°$ show the same tendency as those of the entire wavenumber space in Panel (a). Panel (c) shows that the numerical errors of scheme 1 at $\theta = 45°$ are smaller than or the same as those of Sekido23 at the all Courant numbers. The numerical errors of scheme 2 at $\theta = 45°$ are smaller than or the same as those of Sekido23 except for $0.64 < C < 0.8$.

Figure 2 shows the dependence of the phase velocity errors on wavenumber at $C = 1$ with Sekido23, schemes 1 and 2. The horizontal axis is the wavenumber $k_x\Delta x$, and the vertical axis is the wavenumber $k_y\Delta y$. At $\theta = 45°$ (i.e., $k_x = k_y$), the phase velocity errors of the present schemes are smaller than those of Sekido23. At $\theta = 0°$ (i.e., $k_y = 0$), however, the phase velocity errors of the present schemes are almost the same as those of Sekido23.

3.2. Numerical Error in Three Dimensions

The phase velocity errors of the present schemes are compared with those of FDTD(2,6) and Sekido23 in three dimensions. Figure 3 shows the mean values of the phase velocity errors ε as a function of the Courant number C. Panels (a)–(d) show the phase velocity errors in the entire wavenumber space, at $(\theta, \phi) = (0°, 0°)$, at $(\theta, \phi) = (45°, 0°)$ and at $(\theta, \phi) = (45°, 45°)$, respectively. Here, θ and ϕ are zenith and azimuth angles, respectively. The black, red, green, and blue lines show the numerical errors with FDTD(2,6), Sekido23, schemes 1 and 2 with the optimal coefficients in Tables 3 and 4, respectively.

The Courant conditions are relaxed for large Courant numbers where FDTD(2,6) is unstable. Panel (a) shows that the numerical errors of scheme 2 are smaller than those of the other schemes. The numerical errors of scheme 1 are smaller than or the same as those of FDTD(2,6) and Sekido23 for $C < 0.9$.

TABLE 3. Optimal coefficients for scheme 1 in the three dimensions.

C	α	C	α
0.40	−0.0132	0.71	0.1417
0.41	−0.0054	0.72	0.1414
0.42	0.0019	0.73	0.141
0.43	0.0089	0.74	0.1405
0.44	0.015	0.75	0.1399
0.45	0.0218	0.76	0.1391
0.46	0.0279	0.77	0.1383
0.47	0.0338	0.78	0.1374
0.48	0.0398	0.79	0.1365
0.49	0.0462	0.80	0.1355
0.50	0.0582	0.81	0.1346
0.51	0.0704	0.82	0.1337
0.52	0.0811	0.83	0.1329
0.53	0.0905	0.84	0.1321
0.54	0.0987	0.85	0.1313
0.55	0.1059	0.86	0.1306
0.56	0.1121	0.87	0.1299
0.57	0.1175	0.88	0.1292
0.58	0.1221	0.89	0.1286
0.59	0.1261	0.90	0.128
0.60	0.1294	0.91	0.1274
0.61	0.1323	0.92	0.1268
0.62	0.1347	0.93	0.1263
0.63	0.1366	0.94	0.1258
0.64	0.1382	0.95	0.1253
0.65	0.1395	0.96	0.1248
0.66	0.1404	0.97	0.1244
0.67	0.1411	0.98	0.1239
0.68	0.1416	0.99	0.1235
0.69	0.1418	1.00	0.1231
0.70	0.1418		

TABLE 4. Sets of optimal coefficients for scheme 2 in the three dimensions.

C	α	β	C	α	β
0.40	0.3618	0.9847	0.71	0.0008	−0.1068
0.41	0.3401	0.8626	0.72	0.0039	−0.1021
0.42	0.3192	0.7539	0.73	0.0209	−0.0868
0.43	0.2989	0.6565	0.74	0.0346	−0.0746
0.44	0.2787	0.568	0.75	0.0488	−0.0626
0.45	0.2582	0.4866	0.76	0.0583	−0.0543
0.46	0.2366	0.4098	0.77	0.0696	−0.0451
0.47	0.2123	0.334	0.78	0.0806	−0.0365
0.48	0.1721	0.2337	0.79	0.0886	−0.0302
0.49	0.1164	0.1124	0.80	0.0959	−0.0246
0.50	0.0693	0.0164	0.81	0.1051	−0.0179
0.51	0.0256	−0.0649	0.82	0.113	−0.0124
0.52	−0.0103	−0.1271	0.83	0.1189	−0.0082
0.53	−0.0405	−0.1752	0.84	0.118	−0.0082
0.54	−0.066	−0.2121	0.85	0.1248	−0.0038
0.55	−0.0835	−0.235	0.86	0.1289	−0.001
0.56	−0.1079	−0.2632	0.87	0.1363	0.0035
0.57	−0.1178	−0.2717	0.88	0.1392	0.0054
0.58	−0.1286	−0.2796	0.89	0.1427	0.0076
0.59	−0.1353	−0.2817	0.90	0.1478	0.0105
0.60	−0.1423	−0.2832	0.91	0.1507	0.0122
0.61	−0.1378	−0.2723	0.92	0.1536	0.0138
0.62	−0.129	−0.2576	0.93	0.1563	0.0153
0.63	−0.1156	−0.2389	0.94	0.1607	0.0175
0.64	−0.1018	−0.2207	0.95	0.1617	0.018
0.65	−0.092	−0.2069	0.96	0.1642	0.0193
0.66	−0.0739	−0.1861	0.97	0.1661	0.0202
0.67	−0.0542	−0.1647	0.98	0.167	0.0206
0.68	−0.0399	−0.1489	0.99	0.1678	0.021
0.69	−0.03	−0.1374	1.00	0.1699	0.0219
0.70	−0.0166	−0.1235			

Panels (b), (c), and (d) show that the numerical errors at $(\theta, \phi) = (45°, 45°)$ are the smallest among the three directions. Panels (b) and (c) show that the numerical errors of schemes 1 and 2 at $(\theta, \phi) = (0°, 0°)$ and $(\theta, \phi) = (45°, 0°)$ show the same tendency as those of the entire wavenumber space in Panel (a). Panel (d) shows that the numerical errors of scheme 1 at $(\theta, \phi) = (45°, 45°)$ are smaller than or the same as those of Sekido23 except for $0.85 < C$. The numerical errors of scheme 2 at $(\theta, \phi) = (45°, 45°)$ are smaller than or the same as those of Sekido23 except for $0.51 < C < 0.7$.

Figure 4 shows the dependence of the phase velocity errors on wavenumber in the $k_x - k_y$ and $k_r - k_z$ planes at $C = 1$. Here, we define the $x = y$, $z = 0$ line as axis "r" ($(\theta, \phi) = (45°, 0°)$). At small wavenumbers, the phase velocity errors of scheme 1 are smaller than those of Sekido23 and scheme 2. At large wavenumbers, the phase velocity errors of scheme 2 are smaller than those of Sekido23 and scheme 1.

4. NUMERICAL RESULTS

4.1. Numerical Tests in Two Dimensions

Test simulations are performed with the same conditions as the previous study [21]. The following current density is imposed in the same way as the previous study [21]:

$$
\begin{aligned}
J_x\left(x = \frac{\Delta x}{2}, y = 0, z = 0, t\right) &= \cosh^{-2}\left(\frac{t-4}{2\tau}\right) \\
J_x\left(x = \frac{\Delta x}{2}, y = \Delta y, z = 0, t\right) &= -\cosh^{-2}\left(\frac{t-4}{2\tau}\right) \\
J_y\left(x = \Delta x, y = \frac{\Delta y}{2}, z = 0, t\right) &= \cosh^{-2}\left(\frac{t-4}{2\tau}\right) \\
J_y\left(x = 0, y = \frac{\Delta y}{2}, z = 0, t\right) &= -\cosh^{-2}\left(\frac{t-4}{2\tau}\right) \quad (9)
\end{aligned}
$$

where $\tau = 0.15$.

Figure 5 shows the results of numerical simulations with Sekido23, schemes 1 and 2 in two dimensions. Panels (a)–(i) show the spatial profiles of the magnetic field B_z component with $C = 0.7$ and 1.

With $C = 0.7$ and 1, the numerical simulations with both schemes 1 and 2 are performed stably as well as Sekido23. Panels (a)–(c) show that the numerical oscillations with scheme 2 are smaller, and the waveform is closer to the exact waveform than those with the other schemes at $C = 0.7$. The differences between the theoretical speed of light and numerical

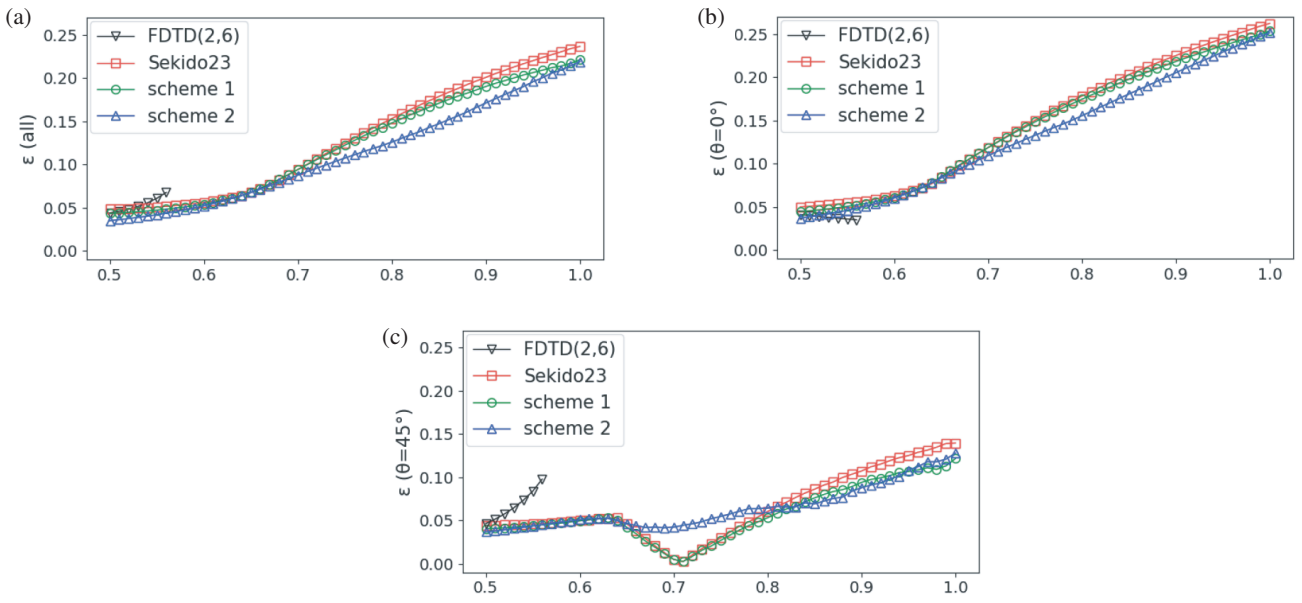

FIGURE 1. The mean values of the two-dimensional phase velocity errors: (a) in the entire wavenumber space; (b) at $\theta = 0°$; (c) at $\theta = 45°$.

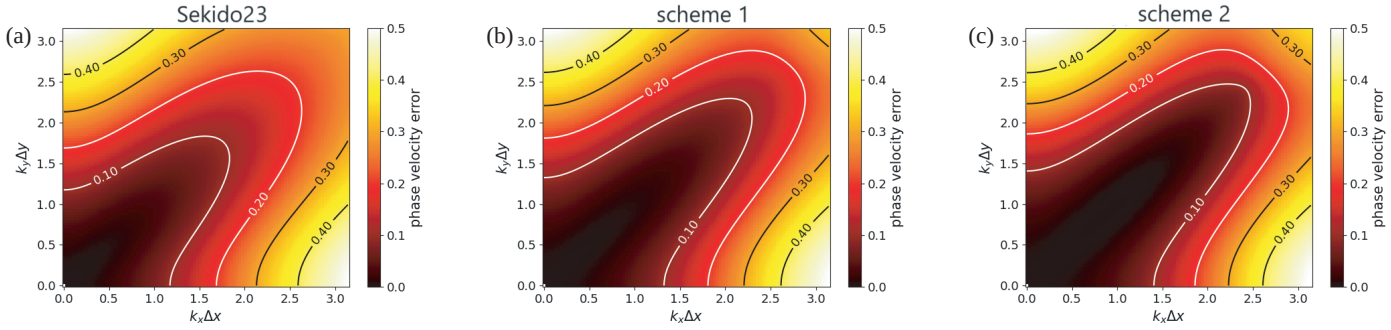

FIGURE 2. Dependence of the phase velocity errors on wavenumber at $C = 1$ in two dimensions: (a) Sekido23; (b) scheme 1; (c) scheme 2.

phase velocities, which depend on wavenumbers, are the cause of the numerical oscillations. However, as seen in Panels (d)–(f), there is little difference in the waveform due to the numerical oscillations among the three schemes at $C = 1$. Panels (a)–(f) show that the numerical oscillations at $\theta = 45°$ are smaller than those at $\theta = 0°$ with $C = 0.7$ and 1. Panels (b) and (c) in Figure 1 show that the phase velocity errors at $\theta = 45°$ are smaller than those at $\theta = 0°$ at $C = 0.7$ and 1. Therefore, the results of the numerical tests are consistent with the numerical errors in phase velocity.

Table 5 shows the computational time of the simulations with $C = 0.5$ and 1. In the same way as [21], the computational time is measured on a single core of the Intel Xeon Gold 6230R processor. The Intel Fortran compiler Version 2021.5.0 is used with options of "-ipo -ip -O3 -xCASCADELAKE".

The computational time with $C = 0.5$ is two times of that with $C = 1$. At the same Courant number, the computational time increases as the number of operations increases. With $C = 0.5$, the computational times with schemes 1 and 2 are 1.21 and 1.53 times longer than that with Sekido23, respectively, although schemes 1 and 2 have 1.625 and 2.375 times larger number of operations than Sekido23, respectively. The total computational time is given by the sum of the processing time and the memory access time.

TABLE 5. Computational time of the two-dimensional simulations.

	$C = 0.5$	$C = 1$
Sekido23	1.51422649439424	0.756914421655238
scheme 1	1.83647139837965	0.920353360809386
scheme 2	2.31595435785130	1.15252507405356

4.2. Numerical Tests in Three Dimensions

Test simulations are performed with the same conditions as the previous study [21]. Figure 6 shows the results of numerical simulations with Sekido23, schemes 1 and 2 in three dimensions. Panels (a)–(l) show the spatial profiles of the magnetic field B_z component with $C = 0.7$ and 1.

With $C = 0.7$ and 1, the numerical simulations with both scheme 1 and 2 are performed stably as well as Sekido23. Panels (a)–(f) show that the numerical oscillations with scheme 2

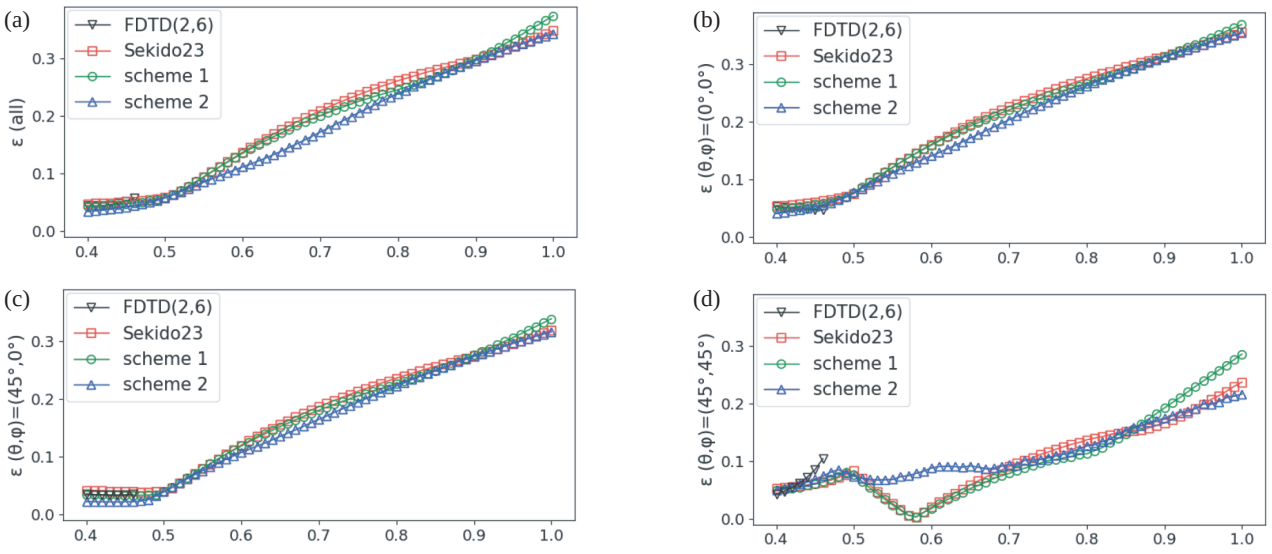

FIGURE 3. The mean values of the three-dimensional phase velocity errors: (a) in the entire wavenumber space; (b) at $(\theta, \phi) = (0°, 0°)$; (c) at $(\theta, \phi) = (45°, 0°)$; (d) $(\theta, \phi) = (45°, 45°)$.

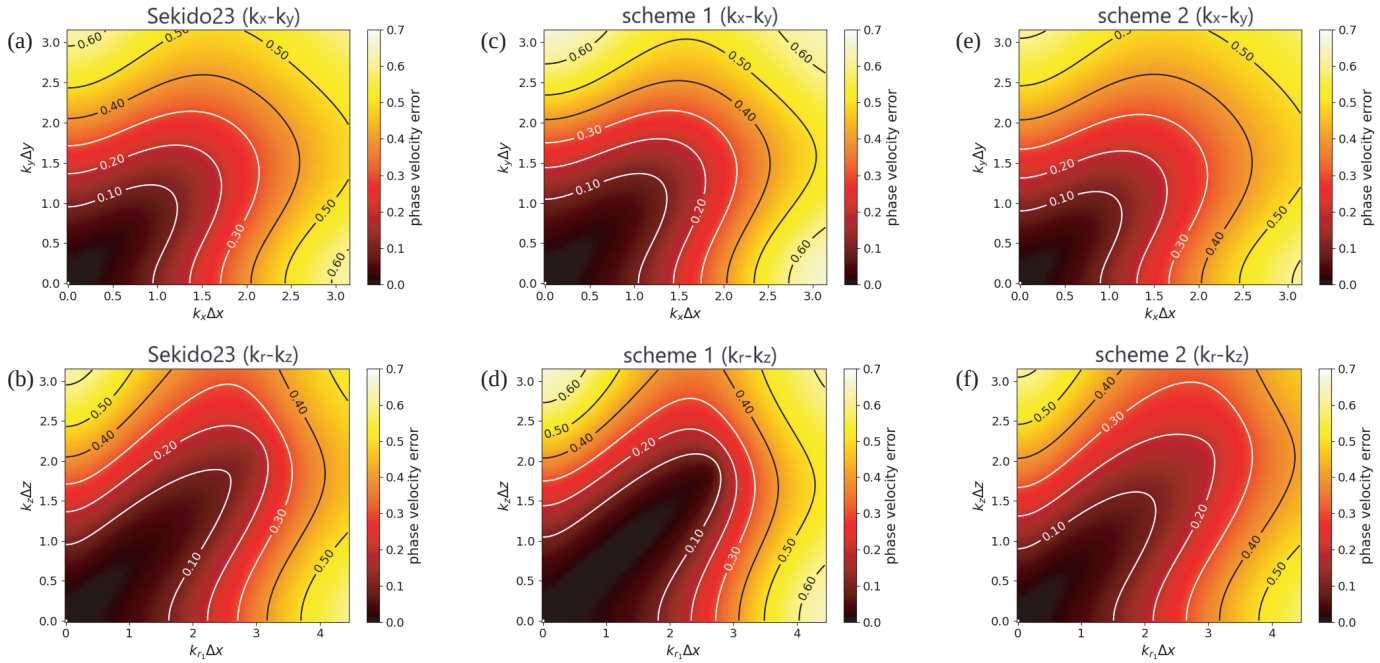

FIGURE 4. Dependence of the phase velocity errors on wavenumber at $C = 1$ in two dimensions: (a) Sekido23 in the k_x-k_y plane; (b) scheme 1 in the k_x-k_y plane; (c) scheme 2 in the k_x-k_y plane; (d) Sekido23 in the k_r-k_z plane; (e) scheme 1 in the k_r-k_z plane; (f) scheme 2 in the k_r-k_z plane.

are smaller, and the waveform is closer to the exact waveform than those with the other schemes at $C = 0.7$. However, as seen in Panels (g)–(l), there is little difference in the waveform due to the numerical oscillations among the three schemes at $C = 1$. The numerical oscillations at $(\theta, \phi) = (45°, 45°)$ are smaller than those at $(\theta, \phi) = (0°, 0°)$ and $(45°, 0°)$. Panels (b)–(d) in Figure 3 show that the numerical errors at $(\theta, \phi) = (45°, 45°)$ are the smallest among the three directions. Therefore, the results of the numerical tests are consistent with the numerical errors in phase velocity.

Table 6 shows the computational time of the simulations with $C = 0.4$ and 1. The computational time with $C = 0.4$ is 2.5 times of that with $C = 1$. At the same Courant number, the computational time increases as the number of operations increases. With $C = 0.4$, the computational time with schemes 1 and 2 are 1.24 and 1.28 times longer than that with Sekido23, respectively, although schemes 1 and 2 have 1.625 and 2.375 times larger number of operations than Sekido23, respectively.

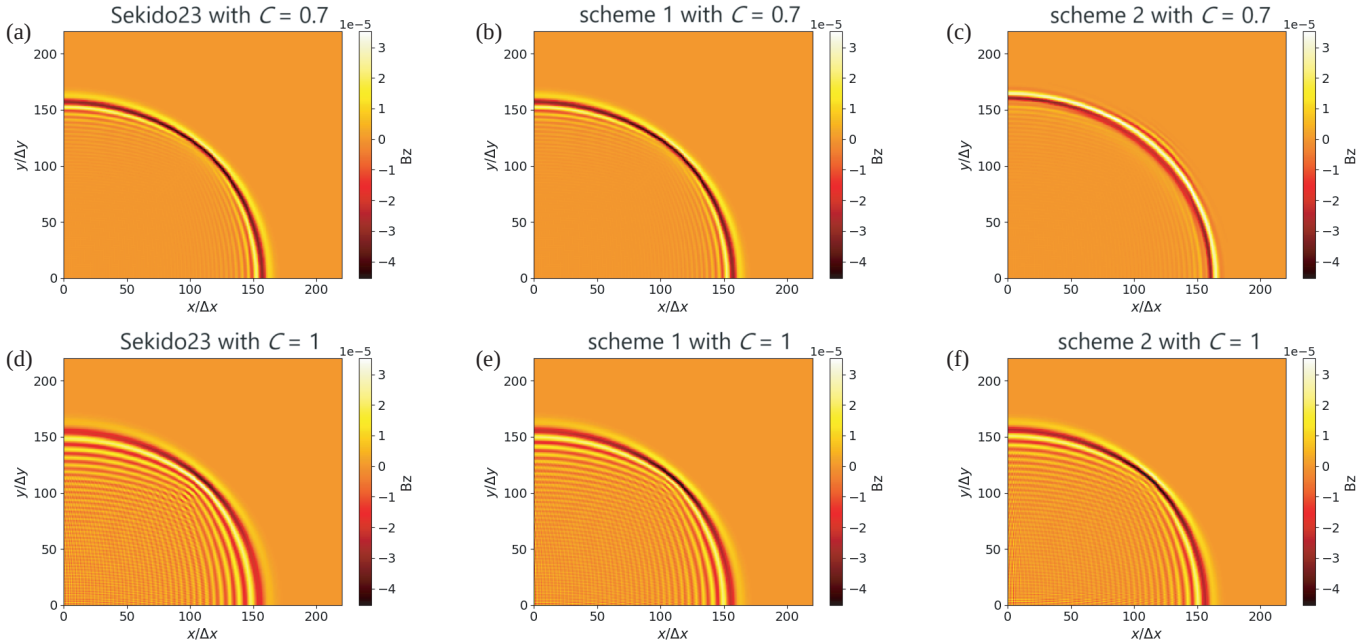

FIGURE 5. Spatial profiles of B_z in two dimensions at $t = 200\Delta t/C$: (a) Sekido23 with $C = 0.7$; (b) scheme 1 with $C = 0.7$; (c) scheme 2 with $C = 0.7$; (d) Sekido23 with $C = 1$; (e) scheme 1 with $C = 1$; (f) scheme 2 with $C = 1$.

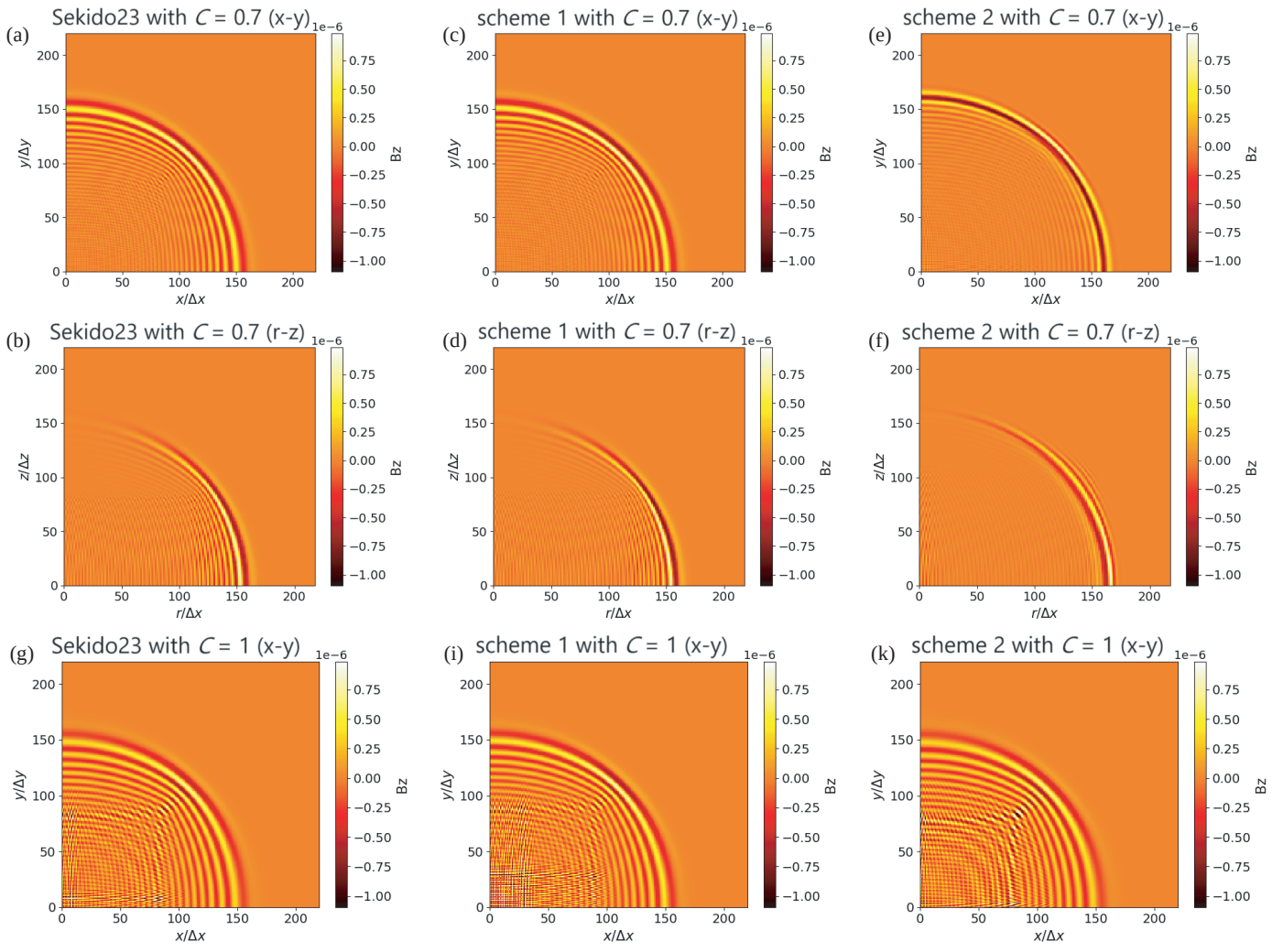

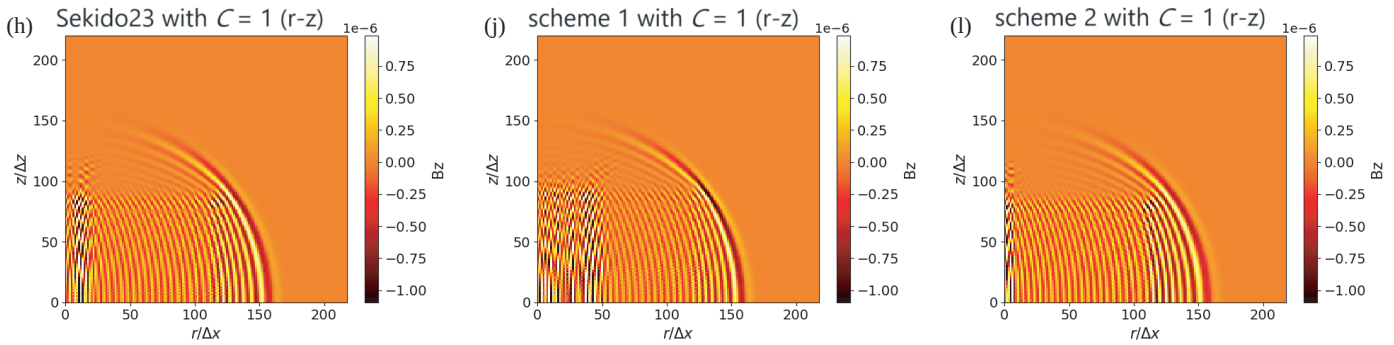

FIGURE 6. Spatial profiles of B_z in three dimensions at $t = 200\Delta t/C$: (a) Sekido23 in the x-y plane with $C = 0.7$; (b) Sekido23 in the r-z plane with $C = 0.7$; (c) scheme 1 in the x-y plane with $C = 0.7$ with $C = 0.7$; (d) scheme 1 in the r-z plane with $C = 0.7$; (e) scheme 2 in the x-y plane with $C = 0.7$ with $C = 0.7$; (f) scheme 2 in the r-z plane with $C = 0.7$; (g) Sekido23 in the x-y plane with $C = 1$; (h) Sekido23 in the r-z plane with $C = 1$; (i) scheme 1 in the x-y plane with $C = 1$; (j) scheme 1 in the r-z plane with $C = 1$; (k) scheme 2 in the x-y plane with $C = 1$; (l) scheme 2 in the r-z plane with $C = 1$.

TABLE 6. Computational time of the three-dimensional simulations.

	$C = 0.4$	$C = 1$
Sekido23	479.554174284451	192.729279914498
scheme 1	592.487470116466	237.065526464768
scheme 2	613.259739442542	245.371084113605

5. CONCLUSION

A new non-dissipative and explicit method is developed for relaxation of the Courant condition in FDTD(2,6). The FDTD(2,6) method is not used commonly, because its Courant condition is too restricted. In the present study, third- and fifth-degree spatial difference terms are appended to the time-development equations of FDTD(2,6) with coefficients in the same way as our previous study [21].

A coefficient search is performed by using the dispersion relations for relaxing the Courant condition and minimizing the mean value of the phase velocity errors in the whole wavenumber space. The present schemes are stable with large Courant numbers up to $C = 1$ as the previous study [21].

The numerical errors of the present schemes are smaller than those of FDTD(2,6) with small Courant numbers. For large Courant numbers, the numerical errors of FDTD(2,6) with the fourth-order third-degree difference terms only are not reduced substantially from those of FDTD(2,4) with the second-order third-degree terms. This is because the Courant condition of FDTD(2,6) is more restricted than that of FDTD(2,4).

The FDTD(2,6) scheme with the third- and fifth-degree differences have smaller phase velocity errors than FDTD(2,6) with third-degree difference only. However, numerical oscillations with the present schemes based on FDTD(2,6) have almost the same amplitude as those with the previous scheme based on FDTD(2,4). There remains a large anisotropy in the phase velocity errors with one-dimensional higher-degree difference terms. Therefore, a straightforward extension of the present scheme to FDTD(2,8) is not effective.

ACKNOWLEDGEMENT

This work was supported by the Ministry of Education, Culture, Sports, Science and Technology (MEXT)/Japan Society for the Promotion of Science (JSPS) under Grant-In-Aid (KAKENHI) for Scientific Research (B) No. JP19H01868. Computations of this work were performed on the Center for Integrated Data Science (CIDAS) computer system at the Institute for Space-Earth Environmental Research, Nagoya University as a computational joint research program.

REFERENCES

[1] Yee, K., "Numerical solution of initial boundary value problems involving Maxwell's equations in isotropic media," *IEEE Transactions on Antennas and Propagation*, Vol. 14, No. 3, 302–307, 1966.

[2] Taflove, A., "Application of the finite-difference time-domain method to sinusoidal steady-state electromagnetic-penetration problems," *IEEE Transactions on Electromagnetic Compatibility*, Vol. 22, No. 3, 191–202, 1980.

[3] Fang, J., "Time domain finite difference computation for Maxwell's equations," Ph.D. dissertation, Ph.D. Thesis, Department of Electrical Engineering and Computer Science, University of California, Berkeley, 1989.

[4] Petropoulos, P. G., "Phase error control for FD-TD methods of second and fourth order accuracy," *IEEE Transactions on Antennas and Propagation*, Vol. 42, No. 6, 859–862, 1994.

[5] Weiland, T., "Time domain electromagnetic field computation with finite difference methods," *International Journal of Numerical Modelling: Electronic Networks, Devices and Fields*, Vol. 9, No. 4, 295–319, 1996.

[6] Thoma, P. and T. Weiland, "Numerical stability of finite difference time domain methods," *IEEE Transactions on Magnetics*, Vol. 34, No. 5, 2740–2743, 1998.

[7] Zhou, L., F. Yang, and H. Zhou, "A novel efficient nonstandard high-order finite-difference time-domain method based on dispersion relation analysis," *Electromagnetics*, Vol. 35, No. 1, 59–74, 2015.

[8] Sun, C. and C. W. Trueman, "Unconditionally stable Crank-Nicolson scheme for solving two-dimensional Maxwell's equations," *Electronics Letters*, Vol. 39, No. 7, 595–597, 2003.

[9] Yang, Y., R. S. Chen, and E. K. N. Yung, "The unconditionally stable Crank Nicolson FDTD method for three-dimensional Maxwell's equations," *Microwave and Optical Technology Letters*, Vol. 48, No. 8, 1619–1622, 2006.

[10] Chen, W.-J., P. Ma, and J. Tian, "A novel ADE-CN-FDTD with improved computational efficiency for dispersive media," *IEEE Microwave and Wireless Components Letters*, Vol. 28, No. 10, 849–851, 2018.

[11] Namiki, T., "A new FDTD algorithm based on alternating-direction implicit method," *IEEE Transactions on Microwave Theory and Techniques*, Vol. 47, No. 10, 2003–2007, 1999.

[12] Cooke, S. J., M. Botton, T. M. Antonsen, Jr., and B. Levush, "A leapfrog formulation of the 3-D ADI-FDTD algorithm," *International Journal of Numerical Modelling: Electronic Networks, Devices and Fields*, Vol. 22, No. 2, 187–200, 2009.

[13] Wang, X.-H., W.-Y. Yin, and Z. Z. (David) Chen, "One-step leapfrog ADI-FDTD method for simulating electromagnetic wave propagation in general dispersive media," *Optics Express*, Vol. 21, No. 18, 20 565–20 576, 2013.

[14] Xie, G., Z. Huang, M. Fang, and X. Wu, "A unified 3-D ADI-FDTD algorithm with one-step leapfrog approach for modeling frequency-dependent dispersive media," *International Journal of Numerical Modelling: Electronic Networks, Devices and Fields*, Vol. 33, No. 2, e2666, 2020.

[15] Hadi, M. F. and M. Piket-May, "A modified FDTD(2, 4) scheme for modeling electrically large structures with high-phase accuracy," *IEEE Transactions on Antennas and Propagation*, Vol. 45, No. 2, 254–264, 1997.

[16] Cole, J. B., "High accuracy solution of Maxwell's equations using nonstandard finite differences," *Computers in Physics*, Vol. 11, No. 3, 287–292, 1997.

[17] Cole, J. B., "A high-accuracy realization of the Yee algorithm using non-standard finite differences," *IEEE Transactions on Microwave Theory and Techniques*, Vol. 45, No. 6, 991–996, 1997.

[18] Kudo, H., T. Kashiwa, and T. Ohtani, "Numerical dispersion and stability condition of the nonstandard FDTD method," *Electronics and Communications in Japan (Part II: Electronics)*, Vol. 85, No. 1, 22–30, 2002.

[19] Yang, B. and C. A. Balanis, "An isotropy-improved nonstandard finite-difference time-domain method," *IEEE Transactions on Antennas and Propagation*, Vol. 54, No. 7, 1935–1942, 2006.

[20] Ohtani, T., K. Taguchi, T. Kashiwa, Y. Kanai, and J. B. Cole, "Nonstandard FDTD method for wideband analysis," *IEEE Transactions on Antennas and Propagation*, Vol. 57, No. 8, 2386–2396, 2009.

[21] Sekido, H. and T. Umeda, "Relaxation of the courant condition in the explicit finite-difference time-domain method with higher-degree differential terms," *IEEE Transactions on Antennas and Propagation*, Vol. 71, No. 2, 1630–1639, 2023.